Design and Implementation of an E-Textile SSPP-Based Low-Pass Filter for Advanced Wearable Applications

Jayshri Kulkarni
Dept. of Electrical & Computer Engineering
Wentworth Institute of Technology
Boston, MA, USA
kulkarnij@wit.edu

Jack H Engdahl
Dept. of Mechanical Engineering
Wentworth Institute of Technology
Boston, MA, USA
engdahlj1@wit.edu

Gabrielle J Quintiliani
Dept. of Electrical & Computer Engineering
Wentworth Institute of Technology
Boston, MA, USA
quintilianig@wit.edu

Jose Alcala-Medel
Dept. of Electrical & Computer Engineering
Baylor University
Waco, TX, USA
Jose_Alcala-Medel1@baylor.edu

Douglas E Dow
Dept. of Electrical & Computer Engineering
Wentworth Institute of Technology
Boston, MA, USA
dowd@wit.edu

Yang Li
Dept. of Electrical & Computer Engineering
Baylor University
Waco, TX, USA
yang_li1@baylor.edu

***Abstract*—This paper presents the design and implementation of an electronic textile (e-textile) low-pass filter (LPF) based on Spoof Surface Plasmon Polaritons (SSPPs), achieving a cutoff frequency of 6.47 GHz for advanced wearable applications. The proposed filter comprises m-shaped unit cells designed to be patterned on the top side of a denim substrate, complemented by a complete ground plane on the back side. The dimensions of the filter are $2.15\lambda_0 \times 0.539\lambda_0 \times 0.034\lambda_0$, where λ_0 is the wavelength corresponding to the cutoff frequency. Simulation results reveal a passband frequency range extending from 0 GHz to 6.47 GHz, with a -10 dB impedance bandwidth of 6.47 GHz and a stopband attenuation of -45 dB at 6.90 GHz. The filter demonstrates low insertion loss within the passband, with a maximum value of just 0.8 dB. Finally, the Specific Absorption Rate (SAR) values of 0.0268 W/kg and 0.0125 W/kg for both the 1g and 10g standards, respectively indicate compliance with safety regulations, affirming its suitability for wearable applications on the human body. The e-textile design and SAR analysis ensure that the filter remains both flexible and comfortable, making it well-suited for integration into smart clothing and other wearable devices.**

Keywords— e-textile, Spoof Surface Plasmon Polaritons (SSPP), denim, cutoff frequency, SAR.

I. Introduction

Surface Plasmon Polaritons (SPPs) are electromagnetic waves that propagate along the interface between a metal and a dielectric, arising from the interaction between photons and the free electrons within the metal. In the optical domain, SPPs leverage the metal's negative dielectric constant, which facilitates strong current confinement and effective propagation of these waves. This fundamental characteristic has rendered SPPs highly advantageous for a wide array of optical devices and applications including sensors, imaging systems, and advanced waveguides [1–4].

However, in the terahertz (THz) and microwave frequency bands, conventional metals do not demonstrate the required plasma-like behavior. Instead, they behave as perfect electrical conductors (PECs) possessing positive dielectric constants, which makes the direct excitation of SPPs impractical [5]. To overcome this limitation, the concept of Spoof Surface Plasmon Polaritons (SSPPs) has been introduced. SSPPs are specifically engineered to replicate the characteristics of traditional SPPs while functioning effectively within the THz and microwave frequency ranges.

SSPPs are typically excited using structured metallic surfaces characterized by periodic patterns, which may include pinholes, serpentine slots, meander lines, or fractal geometries. These meticulously designed structures are intended to induce effective surface plasmon resonances at frequencies where traditional SPPs cannot be activated. The periodic arrangement on the metal surface facilitates plasmonic behavior, thereby enabling wave propagation that exhibits characteristics similar to those of SPPs [6–8]. The ability to generate SSPPs in these lower frequency ranges has led to their application in variety of devices and technologies. SSPP-based structures have been successfully incorporated into microwave and THz components, including antennas [9–12], waveguides [13–14], and several types of filters [15–20]. These applications leverage the unique propagation and attenuation properties of SSPPs, presenting new opportunities for advanced electromagnetic devices and systems.

Among the diverse applications of SSPP structures, planar band-pass and low-pass SSPP filters operating within the microwave frequency range are currently significant areas of research. For instance, a proposed low-pass SSPP filter in [15] features single-sided tilted metallic strips with slots, achieving a cutoff frequency of 5.76 GHz and dimensions of $0.75 \times 0.12\ \lambda_0^2$, where λ_0 represents the wavelength at the cutoff frequency of 5.76 GHz. In reference [16], hook-shaped unit cells in conjunction with a full ground plane were utilized in a low-pass SSPP filter designed for operation at 2.45 GHz. Another study, as cited in reference [17], focused on a filter with an electrical size of $1.31 \times 0.19\ \lambda_0^2$, which operates within the frequency range of 0 to 4.50 GHz by integrating meander-shaped unit cells. A compact filter presented in reference [18] employs L-shaped grooves, effectively lowering the cutoff

frequency and achieving a passband range of 26.5 GHz to 29.5 GHz, making it suitable for fifth generation (5G) applications. Moreover, the authors in reference [19] introduced a double-layered, flexible low-pass filter featuring inverted triangular unit cells on both sides of the substrate. This filter achieved a cutoff frequency of 7.15 GHz, with physical dimensions measuring 1.225 $\lambda_0 \times 0.175$ $\lambda_0 \times 0.006$ λ_0. Reference [20] describes a low-pass filter utilizing double-layered SSPPs that features a cutoff frequency of 4.83 GHz, incorporating interdigital strips that significantly enhance the compactness of the layout, which measures only 1.51 $\lambda_0 \times 0.21$ λ_0.

This paper introduces a flexible, compact wideband Low-Pass Filter (LPF) based on SSPP technology, utilizing m-shaped unit cells arranged in a tapering configuration. This filter was designed to be placed on the top side of a denim substrate, achieving a cutoff frequency of 6.47 GHz. By incorporating unequal lengths in the arms of the different m-shaped unit cell, the design facilitates smaller dimensions for the filter and a reduced width for the transmission line. This design effectively covers a passband frequency range of 0 to 6.47 GHz. This study investigates and analyzes the effects of varying the dimensional parameters of the unit cell of SSPP LPF on both the cutoff frequency and bandwidth of the filter. Finally, the Specific Absorption Rate (SAR) analysis confirmed that the proposed filter design is safe for wearable body applications.

II. Unit Cell Design and Dispersion Curve

The geometric design of the m-shaped SSPP unit cell measuring 15 × 8 mm^2 is illustrated in Fig. 1a, accompanied by its corresponding dispersion curve presented in Fig. 1b. The unit cell was designed on a denim substrate characterized by a dielectric constant (ε_r), loss tangent (tanδ), and thickness of 1.6, 0.025, and 1.6 mm, respectively. A copper layer serving as a conductive element, had a thickness of 0.018 mm and was utilized for both patterning the cell and constructing the ground plane. The key parameters of the design included the dimensional parameter of the height of the m-shaped cell (u_5), the width of the transmission line (u_3), and the width of the arms of the m-shaped cell (u_9), as well as the periodicity (p). These parameters were optimized using CST Microwave Studio, Dassault System, Paris, France. These parameters are listed in Table I.

To evaluate the performance of the SSPP LPF structure, the dispersion properties of the proposed unit cell were analyzed. Simulations of the dispersion diagram for an infinitely long transmission line were conducted using the Eigenmode solver in CST Microwave Studio with periodic boundary conditions. The resulting dispersion curve is displayed in Fig. 1b. As indicated in the curve, the dispersion approaches an asymptotic frequency at 6.47 GHz, highlighting the operational limits of the SSPP filter.

TABLE I. Optimized Dimensional Parameters of Unit Cell

Parameter	Value (mm)	Parameter	Value (mm)
u_1	8	u_6	2
u_2	15	u_7	2
u_3	4	u_8	1
u_4	8	u_9	1
u_5	9	p	8

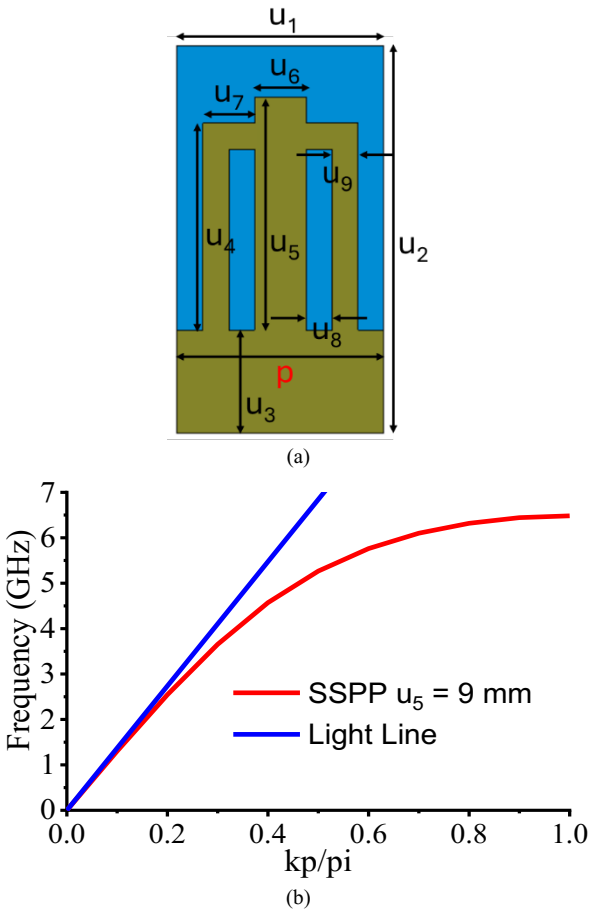

Fig. 1. (a) Geometric design (b) simulated dispersion curve.

To investigate the impact of the height (u_5) of the proposed unit cell on the asymptotic frequency, a parametric study was conducted, and the corresponding dispersion curves are presented in Fig. 2. The data indicates that as 'u_5' increases, the asymptotic frequency decreases. Notably, the cutoff frequency of the proposed unit cell is closely aligned when $u_5 \approx \frac{\lambda_0}{10}$, specifically at u_5 = 9 mm. Setting the height (u_5) of the proposed unit cell at 9 mm effectively reduced the transverse dimensions of the filter, enhanced the wave confinement, and achieved a cutoff frequency of 6.47 GHz. This optimization demonstrated the potential for improved performance in SSPP LPF designs.

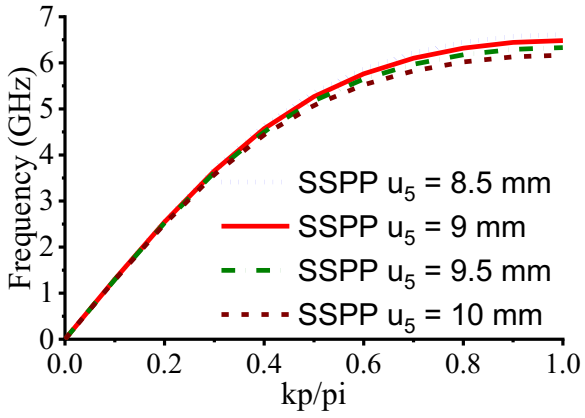

Fig. 2. Dispersion diagrams corresponding to different height (u_5) values.

III. Geometric Configuration of SSPP LPF

The geometric configuration of the flexible, compact SSPP LPF is illustrated in Fig. 3. This design incorporated m-shaped unit cells situated on a denim substrate along with a full ground plane on the backside. The electrical dimensions of the filter were $2.15\lambda_o \times 0.539\lambda_o \times 0.034\lambda_o$, where λ_0, corresponds to the cutoff frequency of 6.47 GHz. As shown in Fig. 3, the entire LPF is divided into three distinct regions: Region 1, located on both sides of the LPF, corresponds to feeding ports 1 and 2 of the microstrip line. This facilitates the transmission of quasi-Transverse Electromagnetic Mode (TEM) within the frequency range of 0 GHz to 6 GHz. Region 2, also positioned on both sides, serves as a matching section that transitions from the microstrip line to the waveguide section. Region 3, situated in the center of the filter and comprising five-unit cells, functions as the waveguide. The dimensions of regions 1, 2, and 3 have been optimized using CST Microwave Studio and are detailed in Table II.

IV. Results and Discussion

The simulated reflection coefficient (S_{11}) and insertion loss (S_{12}), both expressed in decibels (dB), are depicted in Fig. 4. The S_{11} curve indicated that the -10 dB impedance bandwidth spanned from 0 GHz to 6.47 GHz. This aligns with the dispersion characteristics of the unit cell depicted in Fig. 2, thereby confirming a cutoff frequency of 6.47 GHz. Furthermore, the simulated S_{12} remained near 0 dB within the passband, and decreased to -30 dB in the stopband. This behavior demonstrated efficient in-band transmission and excellent out-of-band suppression, highlighting the effectiveness of the SSPP LPF design.

TABLE II. Optimized Dimensional Parameters of SSPP Filter

Parameter	Value (mm)	Parameter	Value (mm)
L	100	d	1
W	25	e	2
a	11	f	2
b	8	g	78
c	1	r	2

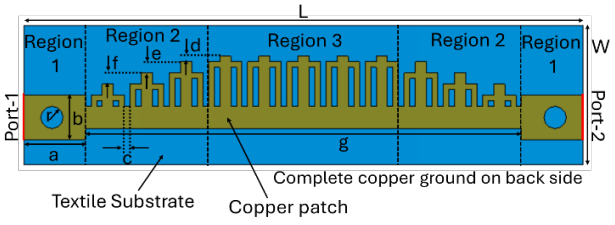

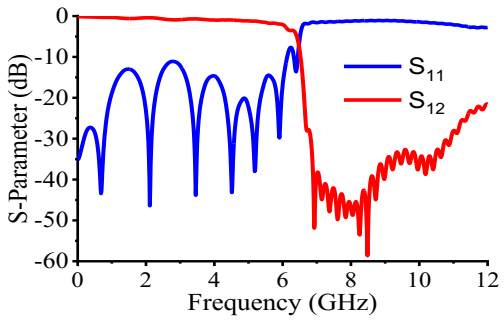

Fig. 4. Simulated S_{11} and insertion loss S_{12} curves of filter.

To gain a deeper understanding of the operating mechanism of the proposed filter, a parametric study was conducted on key parameters, namely 'a', 'b', and 'R'. This study aimed to analyze their effect on the S_{11} and S_{12} responses. Figs. 5, 6, and 7 illustrate the variation of parameters in increments of 0.5 mm.

As observed in Fig. 5, changes in the parameter 'a' significantly impact the S_{11} response within the 2 GHz to 4 GHz frequency range. Specifically for values of 'a' below 11 mm, a reduction in S_{11} below -10 dB is observed, along with a slight reduction in cut-off frequency. Conversely, for values above 11 mm, the cut-off frequency remained relatively constant, and negligible effects were noted in the stopband. Based on these results, the value of 'a' was finalized at 11 mm.

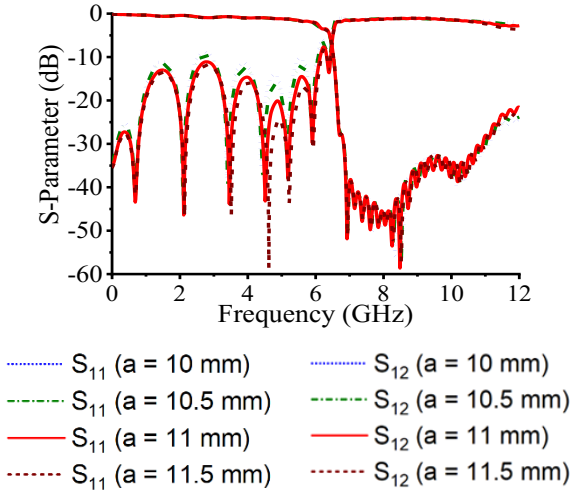

Fig. 5. Simulated S_{11} and S_{12} for varying 'a'.

In Fig. 6, variations in 'b' from 3 mm to 4.5 mm affected both the cutoff frequency and the S_{12} response. For values of 'b' less than 4 mm, a reduction in the cutoff frequency was observed. However, for values above 4 mm the performance of S_{12} deteriorated in the stopband. Therefore, 'b' was selected at 4 mm, where the desired cutoff frequency of 6.47 GHz was achieved.

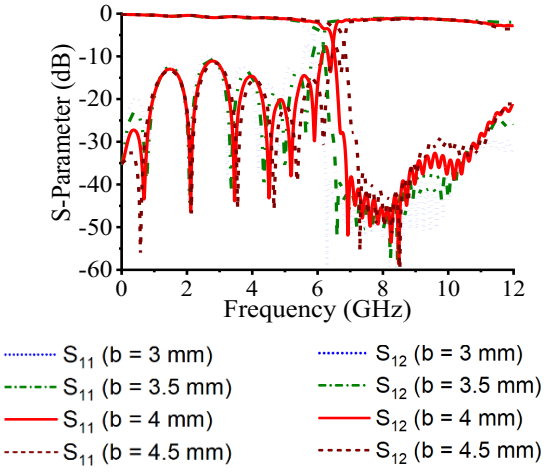

Fig. 6. Simulated S_{11} and S_{12} for varying 'b'.

Finally, as illustrated in Fig. 7, variations in 'r' from 1 mm to 2.5 mm impact the S_{11} response except at r = 2 mm. Therefore, 'r' was chosen as 2 mm, as this value achieved the desired cutoff frequency of 6.47 GHz with S_{11} response well below -10 dB.

To explore the principles of LPF, the electric field distribution in the x-o-y plane of 3.50 GHz and 6.90 GHz is illustrated in Figs. 8 and 9, respectively. As shown in Fig. 8, electromagnetic signal transmission occurs from port 1 to port 2, confirming the passband operation of the filter.

In contrast, Fig. 9 shows the blocking of electromagnetic signal from passing between port 1 and port 2, indicating effective stopband rejection. This validated both the LPF's capability for passband transmission and its efficacy in stopband suppression.

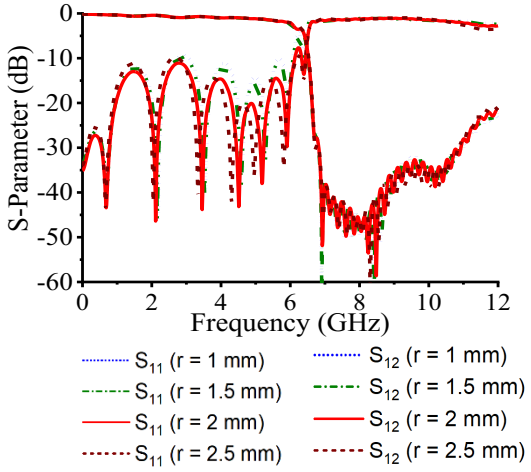

Fig. 7. Simulated S_{11} and S_{12} for varying 'r'.

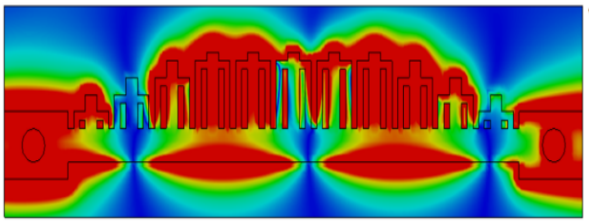

Fig. 8 Electric field distribution at 3.50 GHz (passband).

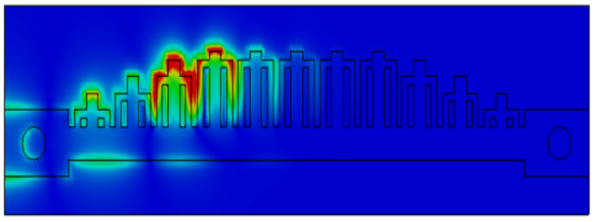

Fig. 9 Electric field distribution at 6.90 GHz (stopband).

V. SAR Analysis

The SAR analysis was essential for evaluating the electromagnetic safety of the proposed filter design. A simplified flat phantom, designed to mimic a human tissue model, was constructed in CST software. The artificial tissue is based on a multilayer structure consisting of skin, fat, and muscle, as shown in Fig. 10. This phantom was positioned 5 mm away from the filter, as it might occur for denim fabric being worn.

The simulation was conducted over a frequency range of 0 GHz to 12 GHz with an input power of 100 mW. At the operating frequency of 6 GHz, the maximum SAR values recorded for the 1 g and 10 g tissue models were 0.0268 W/kg and 0.0125 W/kg, respectively as shown in Fig. 11. These values are significantly below the safety limits of 1.6 W/kg for 1 g tissue and 2 W/kg for 10 g tissue. Therefore, these findings support that the filter can be deployed in wearable or on-body applications without posing health risks.

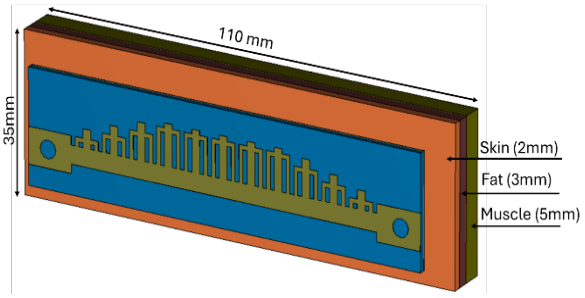

Fig. 10. Flat phantom model for SAR analysis.

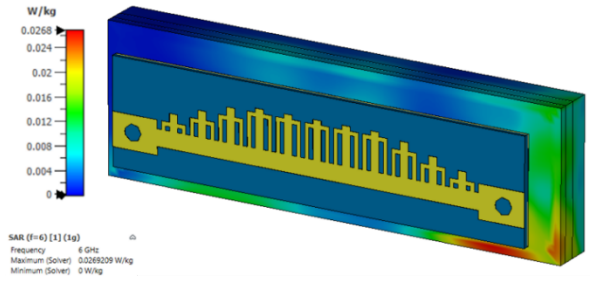

(a)

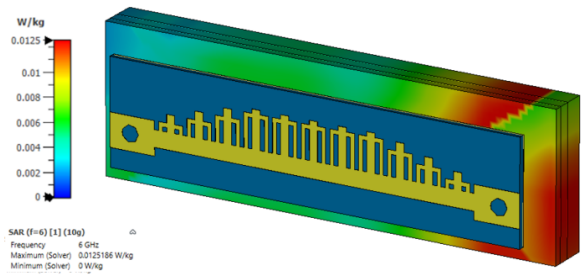

(b)

Fig. 11 SAR analysis of proposed SSPP LPF (a) 1g tissue (b) 10g tissue.

TABLE III. COMPARISON WITH OTHER SSPP LOW PASS FILTER FUNCTION IN MICROWAVE BANDS

Ref.	Size ($\lambda_0 x \lambda_0$)	Pass band range (GHz)	S_{11} (dB) in pass band	Out of band suppression (dB)
[15]	$0.7\lambda_0 \times 0.1\lambda_0$	(0-66)	>15dB	>30
[16]	$0.68\lambda_0 \times 0.41\lambda_0$	(0-2.45)	>10 dB	>30
[17]	$1.5\lambda_0 \times 0.21\lambda_0$	(0-4.8)	>15 dB	>25
This work	$2.15\lambda_0 \times 0.539\lambda_0$	(0-6.47)	>10 dB	>40

VI. PERFORMANCE COMPARISON

Table III presents a comparison between the proposed filter and other SSPP low-pass filters operating in the microwave frequency range. The S_{11} (dB) within the passband and the out-of-band attenuation of the proposed filter are comparable to those of other designs. However, the compact size, wide bandwidth of the proposed filter, makes it highly suitable for integration into radio-frequency circuits.

VII. CONCLUSION

The proposed flexible and compact SSPP LPF demonstrated outstanding performance characteristics. With a compact footprint of 100 × 50 mm² and a flexible design utilizing denim as the substrate. This design is suitable for wearable and on-body applications. The filter achieved a wide passband up to 6.47 GHz, with a low insertion loss of -0.8 dB in the passband, ensuring efficient signal transmission. Furthermore, SAR analysis confirmed that the filter operated safely within established electromagnetic exposure limits, with SAR values of 0.0268 W/kg for the 1 g tissue model and 0.0125 W/kg for the 10 g tissue model, both significantly below regulatory thresholds. The flexibility, compactness, and low SAR values make this filter particularly advantageous for integration into clothing, facilitating seamless incorporation into smart textiles and wearable devices while ensuring both comfort and safety.

REFERENCES

[1] D. Gramotnev and S. Bozhevolnyi, "Plasmonics beyond the diffraction limit," *Nature Photon.*, vol. 4, pp. 83–91, 2010.

[2] J. R. Krenn and J. C. Weeber, "Surface plasmon polaritons in metal stripes and wires," *Phil. Trans. Roy. Soc. A Math. Phys. Eng. Sci.*, vol. 362, no. 1817, pp. 739–756, Apr. 2004, doi: 10.1098/rsta.2003.1344.

[3] X. Shen, T. J. Cui, D. Martin-Cano, and F. J. Garcia-Vidal, "Conformal surface plasmons propagating on ultrathin and flexible films," *Proc. Natl. Acad. Sci. U. S. A.*, vol. 110, no. 1, pp. 40–45, Jan. 2013, doi: 10.1073/pnas.1210417110.

[4] Z.-H. Gao, X.-S. Li, M. Mao, C. Sun, F.-X. Liu, L. Zhang, and L. Zhao, "Ultra-Compact Low-Pass Spoof Surface Plasmon Polariton Filter Based on Interdigital Structure," *Micromachines*, vol. 14, no. 9, pp. 1687, 2023, doi: 10.3390/mi14091687.

[5] A. P. Hibbins, B. R. Evans, and J. R. Sambles, "Experimental verification of designer surface plasmons," *Science*, vol. 308, no. 5722, pp. 670–672, Apr. 2005, doi: 10.1126/science.1109043.

[6] W. Hong and H. Xu, "Plasmonics in composite nanostructures," *Materials Today*, vol. 17, no. 8, pp. 372–380, 2014, doi: 10.1016/j.mattod.2014.05.012.

[7] X. Wang, Y. Deng, Q. Li, Y. Huang, Z. Gong, K. B. Tom, and J. Yao, "Excitation and propagation of surface plasmon polaritons on a non-structured surface with a permittivity gradient," *Light Sci. Appl.*, vol. 5, no. 12, p. e16179, Dec. 2016, doi: 10.1038/lsa.2016.179.

[8] R. Lee, B. Wang, and M. A. Cappelli, "Plasma modification of spoof plasmon propagation along metamaterial-air interfaces," *Appl. Phys. Lett.*, vol. 111, p. 261105, 2017, doi: 10.1063/1.5006666.

[9] Y. Wu et al., "Design of Quasi-Endfire Spoof Surface Plasmon Polariton Leaky-Wave Textile Wearable Antennas," *IEEE Access*, vol. 10, pp. 115338–115350, 2022, doi: 10.1109/ACCESS.2022.3218217.

[10] Z. H. Jiang, M. D. Gregory, and D. H. Werner, "Design and Experimental Investigation of a Compact Circularly Polarized Integrated Filtering Antenna for Wearable Biotelemetric Devices," *IEEE Trans. Biomed. Circuits Syst.*, vol. 10, no. 2, pp. 328–338, Apr. 2016, doi: 10.1109/TBCAS.2015.2438551.

[11] L. Liu, M. Chen, and X. Yin, "Single-Layer High Gain Endfire Antenna Based on Spoof Surface Plasmon Polaritons," *IEEE Access*, vol. 8, pp. 64139–64144, 2020, doi: 10.1109/ACCESS.2020.2984153.

[12] Z.-C. Hao, J. Zhang, and L. Zhao, "A compact leaky-wave antenna using a planar spoof surface plasmon polariton structure," *Int. J. RF Microw. Comput. Aided Eng.*, vol. e21617, 2019, doi: 10.1002/mmce.21617.

[13] Z. Wang, H. Feng, X. Yang, X. Xu, Y. Zheng, and L. Ye, "A Windmill-Shaped SSPP Waveguide for High-Efficiency Microwave and Terahertz Propagation," *Electronics*, vol. 11, no. 9, p. 1293, 2022, doi: 10.3390/electronics11091293.

[14] Y. Ye, Z. Chen, C. Wang, J. Zhu, J. Zhuo, and Q. H. Liu, "Compact Spoof Surface Plasmon Polariton Waveguides and Notch Filters Based on Meander-Strip Units," *IEEE Photonics Technol. Lett.*, vol. 33, no. 3, pp. 135–138, Feb. 2021, doi: 10.1109/LPT.2020.3046837.

[15] B. K. Bharti and A. N. Yadav, "A Novel Miniaturized SSPP Based Low Pass Filter with Ultra-Wide-Stopband," *TechRxiv.*, Apr. 2024, doi: 10.36227/techrxiv.171294822.20712586/v1.

[16] J. Alcala-Medel, J. Kulkarni, S. McClain, and Y. Li, "Simulation and measurement of electromagnetic wave propagations along a wearable e-textile metasurface transmission line," *J. Electromagn. Waves Appl.*, vol. 38, no. 14, pp. 1523–1537, 2024, doi: 10.1080/09205071.2024.2378052.

[17] M. Wang, S. Sun, H. F. Ma, and T. J. Cui, "Supercompact and Ultrawideband Surface Plasmonic Bandpass Filter," *IEEE Trans. Microw. Theory Techn.*, vol. 68, no. 2, pp. 732–740, Feb. 2020, doi: 10.1109/TMTT.2019.2952123.

[18] B. Mazdouri, M. M. Honari, and R. Mirzavand, "Miniaturized spoof SPPs filter based on multiple resonators for 5G applications," *Sci. Rep.*, vol. 11, p. 22557, 2021, doi: 10.1038/s41598-021-01944-6.

[19] B. B. Pathak and R. S. Kshetrimayum, "Conformal and Compact Low Pass Filter based on SSPP for B5G NR FR1 Radio Stripe Network Application," in *Proc. 2023 Int. Conf. Microw. Opt. Commun. Eng.*, Bhubaneswar, India, 2023, pp. 1–4, doi: 10.1109/ICMOCE57812.2023.10166095.

[20] X. Zhang, S. Sun, Q. Yu, L. Wang, K. Liao, and S. Liu, "Novel high-efficiency and ultra-compact low-pass filter using double-layered spoof surface plasmon polaritons," *Microw. Opt. Technol. Lett.*, vol. 64, pp. 1056–1061, 2022.